CLIMATOLOGY OF TRANSIENT EDDY ACTIVITY IN THE MACDA REANALYSIS

T. A. Mooring[1] and R. J. Wilson[2], [1]Program in Atmospheric and Oceanic Sciences, Princeton University (tmooring@princeton.edu), [2]NOAA/GFDL.

Introduction: Studies of the dynamics of the Martian atmosphere are currently limited by the lack of global observations of any dynamical variable other than temperature. Attempts have been made to derive some wind information from temperature fields using simple balance relationships (e.g., [1]). A promising alternative approach is to assimilate whatever data are available into a general circulation model, using the GCM to derive any variable of interest (e.g., [2]).

We are conducting studies of transient eddies in the Martian atmosphere, including a survey of their properties in the MACDA assimilated dataset [2] that we intend to use for the evaluation of GCM simulations, which in some cases have demonstrably different variability from that found in observations [3,4]. Much previous literature discusses Martian transient eddies in terms of zonal wavenumber, but the MACDA dataset's gridded and largely spatiotemporally continuous nature allows us to also use several more spatially localized diagnostic techniques that have previously been used to study terrestrial transient eddies but would be difficult to apply to raw temperature retrievals.

Here we present examples of our analyses based on two time periods/regions: Ls = 305-60° of MY24/25 and MY25/26 for the NH and Ls = 0-65° of MY25 and MY26 for the SH. As has been done extensively for Earth and to a lesser extent for Mars GCM simulations [5], we examine eddy variance maps to study the spatiotemporal distribution of eddy activity.

Using a complementary teleconnection map-based approach, we are also able to calculate local phase propagation velocities of transient eddies, including nonzonal components apparently caused by the Martian topography. Such nonzonal eddy propagation is effectively unrepresentable within the zonal wavenumber paradigm, but is apparently key to dust storm initiation and transport [6]. Finally, preliminary examination of groups of teleconnection maps calculated with various lags suggests that the response of the eddies to topography involves deforming around it.

Dataset: MACDA was produced by assimilating MGS TES temperature and dust optical depth retrievals into the UK MGCM [2]. Filtering of the dataset to retain timescales of variability associated with the transient eddies (here defined as 1.3-30 sols) reveals a clear tendency for each hemisphere's eddy activity to occur in the local winter half-year, with a distinct solsticial pause [7] and substantially weaker eddy activity in the SH. This suggests division of the data in each hemisphere into four "seasons": pre- and post-solstice eddy activity periods, the solsticial pause, and a summer with minimal eddy activity. Our NH (SH) time window corresponds to the post- (pre-) solstice eddy season. (There is also evidence of seasonal change within the pre- and post-solstice eddy seasons themselves, which will be a subject of future investigation.)

EKE and Eddy Geopotential Height Fields: For the time windows of interest, we computed maps showing the spatial structures of EKE = $^1/_2$ (u'^2+ v'^2) and the RMS eddy geopotential height at 3, 4.5, and 6 (2, 3, and 4) hPa in the NH (SH). A sample output plot is shown as Fig. 1, and RMS eddy geopotential height is also contoured in Fig. 2. For both hemispheres the spatial structures of the fields are zonally and meridionally modulated but relatively independent of height within the depth range considered. The principal maxima in the SH EKE and RMS eddy geopotential height fields are reasonably colocated, while the NH EKE maximum is upstream of the principal RMS eddy geopotential height maximum (not shown).

Teleconnection-based Eddy Propagation: Following Wallace et al. ([8], section 4c) we derive local eddy phase propagation velocities from eddy surface pressure fields. Results for the NH post-solstice eddy activity period are shown in Fig. 2. A significant nonzonal component of the propagation velocity field is visible, with eddies propagating around the Tharsis bulge and perhaps also Syrtis Major. Similar behavior is seen on the southern flank of Tharsis as well.

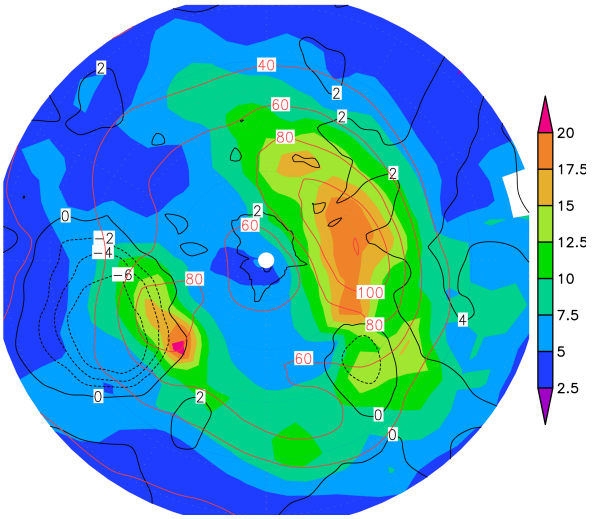

Fig. 1: EKE (shaded, m^2 s^{-2}) and RMS eddy geopotential height (red contours, m) at 3 hPa in the region 20-90°S. Eddy activity is most prominent in the hemisphere 150-330°E. Topography is labeled in km, and 0°E is located at the bottom of the map.

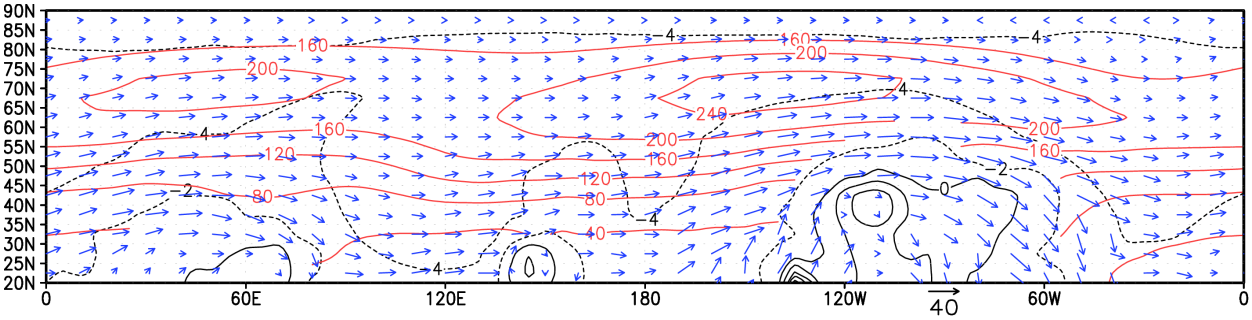

Fig. 2: Eddy phase propagation velocity vectors (arrows) and 6 hPa RMS eddy geopotential height (red contours, m) in the region 20-90°N. Units for the velocity scale arrow are m s^{-1}, and topography is labeled in km.

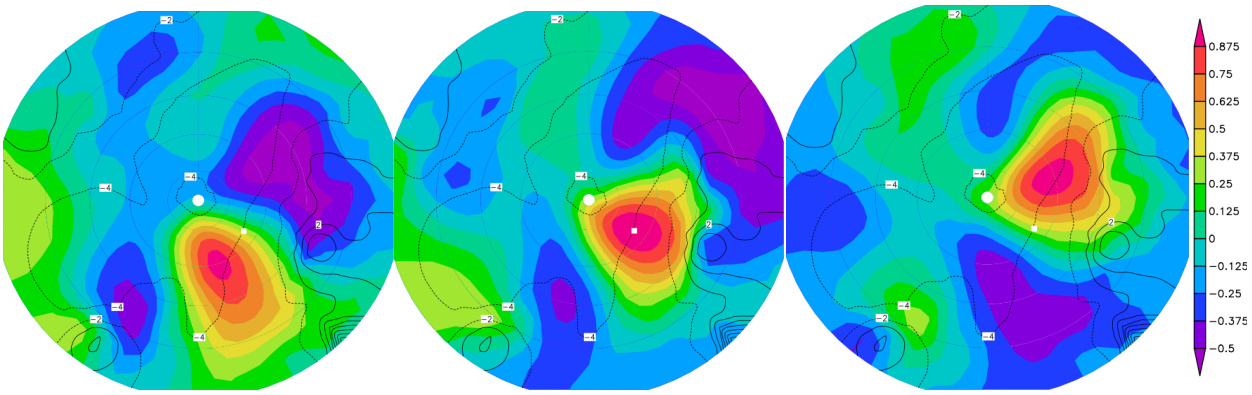

Fig. 3: Teleconnection maps with lags -1, 0, and +1 sols for reference point 67.5°N, 125°W (marked with a white square). The shading indicates the correlation with the reference point, and the "climatological eddy" clearly propagates eastward. Its low zonal wavenumber is qualitatively consistent with spectral analyses of atmospheric data. The maps cover 20-90°N and 180°E is located at the bottom of each map. Topography is labeled in km.

Eddy Horizontal Structure: We can use eddy teleconnection maps (section 3 of [8]) computed from the eddy surface pressure to learn more about the propagation behavior illustrated in Fig. 2. By varying the lag used to compute the teleconnection map, we can see how eddies typically propagate in the vicinity of the map's reference point. Three such teleconnection maps are shown in Fig. 3.

Inspection of sequences of such maps for two NH reference points (67.5°N, 125°W and 47.5°N, 135°E) indicates changes in the characteristic shapes of eddies as they travel in a generally eastward direction. This is presumably to at least some extent driven by interaction of the eddies with topography.

It is not surprising that eddy shapes respond to the topography, given that typical eddy scales are not dramatically different from those of the topography itself. Such deformation of the eddies is quite clearly seen for the 47.5°N, 135°E reference point, as they squeeze around Elysium Mons (not shown).

Discussion: The advent of data assimilation for Mars atmospheric studies represents an opportunity to substantially improve our characterization of the planet's transient eddies, which to date has been little exploited. We have highlighted several aspects of the reanalyzed eddies' behavior that would be obscure in raw temperature retrievals from orbiters, although further assessment of the relationship between reanalysis datasets and actual atmospheric behavior should be conducted. The diagnostic techniques used here avoid assumptions of zonal symmetry, coherence, or propagation and thus represent a step forward in the characterization of zonally asymmetric and nonzonal eddy phenomena. They also represent an additional tool for concisely summarizing transient eddy properties in Mars GCMs, clarifying how they differ from the real Mars as represented in assimilated datasets.

References: [1] Banfield D. G. et al. (2004) *Icarus, 170,* 365-403. [2] Lewis S. R. et al. (2007) *Icarus, 192,* 327-347. [3] Wang H. et al. (2013) *Icarus, 223,* 654-676. [4] Kavulich M. J. et al. (2013) *J. Atmos. Sci., 70,* 3415-3447. [5] Hollingsworth J. L. et al. (1996) *Nature, 380,* 413-416. [6] Wang H. et al. (2005) *JGR, 110,* E07005. [7] Read P. L. et al. (2011) *Fourth Int'l. Wkshp. On the Mars Atmos.,* Paris. [8] Wallace J. M. et al. (1988) *J. Atmos. Sci., 45,* 439-462.